

ePLAS application to plasma jet modeling

R. J. Mason

Research Applications Corporation

Los Alamos, NM 87544

**Plasma Jet Workshop
Los Alamos National Laboratory
Otowi Building
January 24-25, 2008**

*Work performed in part under SBIR Grant No. DE-FG02-07ER84723
for the OFES, Francis Thio, Program Manager

Abstract

- **The ePLAS code provides implicit/hybrid simulation of plasmas spanning large density ranges and large time and spatial scales.**
- **It models plasma components as either Van Leer fluids or PIC particles. The plasma moves in E and B-fields determined by the Implicit Moment Method.**
- **In recent years, code has been applied to the Fast Ignition problem in Inertial Fusion, but in the past its predecessor ANTHEM provided some of the first full-scale modeling of long time scale (microsecond) Plasma Opening Switches for both the Sandia and NRL pulse power programs.**
- **The talk will discuss the emerging new ePLAS capabilities for plasma jets. These include the representation of emitting internal and external electrodes, the capture of electron MHD effects, external circuitry, and field transport in voids.**

We use the RAC ePLAS code

Features:

2-D, *Implicit Moment E&B*-fields, *PIC or fluid* emission (Child Langmuir) electrons, internal and external electrodes, fluid background electrons and ions, relativistic corrections, electron scatter and drag off ions, background (cold) electron resistivity, joule heating, cartesian (x,y) or cylindrical (r,z) geometry.

Special Capabilities:

- **High plasma fill densities (10^{14} - 10^{17} e-/cm³), vacuum regions**
- **No Δt restraint from $\omega_p \Delta t < 1$, global problems**
- **EMHD ($\nu \times B$) B-field penetration modeling.**

Classical collisional treatment includes:

- Scatter done at the Spitzer rate, but modified for low temperatures by a floor (at typically 100 eV) on the background temps.
- Hot electron scatter and drag rates relativistically corrected to match Jackson's and Mosher's analysis.
- Heated cold e^- (from the hot drag and cold scatter) coupled to the ions at a Spitzer rate. When $\nu_{c-i} \approx \nu_{h-c}$ cold heating is directly mirrored in the ions.

References to the methods employed

1. Mason, R. J., “**Heating mechanisms in short-pulse laser-driven cone targets,**” *Phys. Rev. Lett.* **96**, 035001 (2006).
2. Mason, R. J., Dodd, E. S., Albright, B. J., “**Electron transport dependence on target surface conditions and spot size,**” MPo2.15 in IFSA Proceedings (2005), for the J. de Physique.
3. Mason, R. J., Dodd, E. S., and Albright, B. J., “**Electron surface retention in intense short-pulse laser-matter interactions,**” *Phys. Rev. E*, **72**, 015401 (2005).
4. R. J. Mason, “**Implicit hybrid/PIC code ANTHEM,**” in *Proceeding of the 11th International Conference on Emerging Nuclear Energy Systems, ICENES 2002*, p. 284-290, (2002).
6. R. J. Mason and M. Tabak, “**Magnetic field generation in high density laser-matter interactions,**” *Phys. Rev. Lett.* **80**, 524 (1998).
7. R. J. Mason, “**High impedance multi-gap plasma opening switches,**” *IEEE Trans. Plasma Sci.* **23** 465 (1995).
8. M. Tabak, J. Hammer, M. Glinsky, R. Mason et. al., “**Ignition and high gain with ultra-powerful lasers,**” *Phys. of Plasmas*, **1**, 1626 (1994).
9. R. J. Mason, P. Auer, R. N. Sudan, B. Oliver, C. Seyler and J. Greenly, “**Non-linear magnetic field transport in opening switch plasmas,**” *Phys. Fluids B*, **5**, 1115 (1993).
10. R. J. Mason, M. E. Jones, J. M. Grossmann, and P. F. Ottinger “**Magnetic field penetration of erosion switch plasmas,**” *Phys. Rev. Lett.* **61**, 1835 (1988).
11. R. J. Mason, “**An electro-magnetic field algorithm for 2-D implicit plasma simulation,**” *J. Comp. Phys.* **71**, 429 (1987).
12. R. J. Mason and C. Cranfill, “**Hybrid two-dimensional Monte-Carlo electron transport in self-consistent electromagnetic fields,**” *IEEE Trans. Plasma Sci.*, **PS-14**, 45 (1986).

For plasma jets ePLAS includes -

- **Drive circuitry:** an external B-field pushes the jet plasma and drives the wall emission.
- **Load circuitry:** penetrating fields can confront a load beyond the jet.
- **Implicit algorithms for wall emitted electrons,** setting the E-field to zero in conductors.
- **Use of the displacement current and electron inertia to avoid singularities in voids.**

The implicit differencing suppresses plasma wave instability at high densities

Heuristic - for the B=0 limit

$$E^{(m+1)} = E^{(m)} + 4\pi e (n_h v_h^{(m+1)} + n_c v_c^{(m+1)} - Z n_i v_i^{(m+1)}) \Delta t$$

$$v_h^{(m+1)} = \frac{1}{\gamma_h^{(m+1)}} (u_h^{(m)*} - \frac{1}{m_e n_h} \nabla \cdot \bar{P}_h \Delta t - \frac{e}{m_e} E^{(m+1)} \Delta t);$$

v_c and v_i from fluids or particles

$$E^{(m+1)} = \frac{E^{(m)} - 4\pi \sum_{\alpha} \frac{q_{\alpha} n_{\alpha} \Delta t}{\gamma_{\alpha}^{(\oplus)}} (u_{\alpha}^{(m)*} - \frac{1}{m_e n_{\alpha}} \nabla \cdot \bar{P}_{\alpha} \Delta t)}{[1 + \sum_{\alpha} \omega_p^2 (\Delta t)^2 / \gamma_{\alpha}^{(\oplus)}]}$$

level (m) suffices

$$E^{(m)} \Rightarrow -4\pi e \left[\int_0^x (n_h^{(m)} + n_c^{(m)} - Z n_i^{(m)}) \Delta t \right] \leftarrow \text{provides a field correction}$$

for 2D: see JCP '87 ref.

The plasma opening switch presents plasma that can be launched into a jet

VOLUME 61, NUMBER 16

PHYSICAL REVIEW LETTERS

17 OCTOBER 1988

Magnetic Field Penetration of Erosion-Switch Plasmas

Rodney J. Mason and Michael E. Jones

Applied Theoretical Physics Division, Los Alamos National Laboratory, Los Alamos, New Mexico 87545

John M. Grossmann and Paul F. Ottinger

Naval Research Laboratory, Washington, D.C. 20375-5000

(Received 28 June 1988)

**10^{13} e/cm³ plasma
30 ns opening time
3T drive field (MAs)**

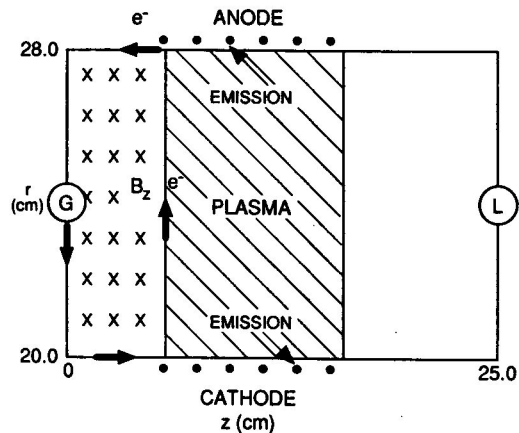
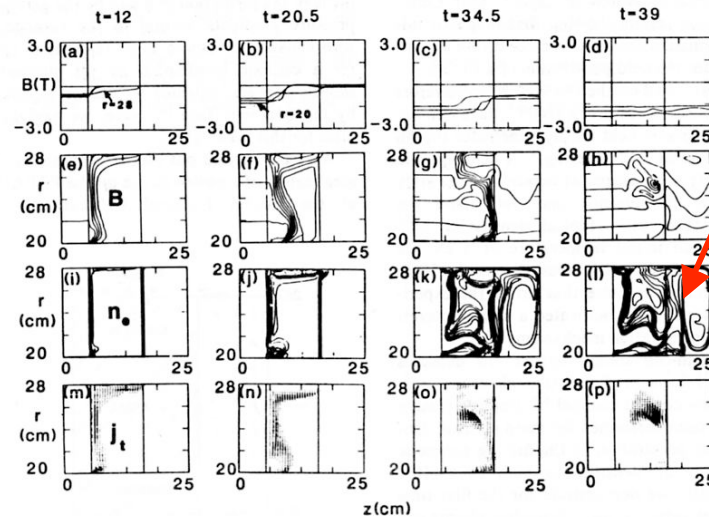


FIG. 1. A generic PEOS for inductive storage. Plasma initially fills the cross-hatched region. G denotes the generator and L the load, here a short circuit.



Emission jets – no load

FIG. 2. Global collisionless calculation of the idealized PBFII PEOS with 10^{13} -cm⁻³ C⁺⁺ fill density, under a linear drive rising to 3 T in 50 ns at the cathode. Frames (a)-(d) (and corresponding columns) are for $t = 12, 20.5, 34.5,$ and 39 ns, respectively. (a)-(d) Linear cuts of $B_z(r,z)$ at $r = 20$ (cathode), 24 (body center), and 28 (anode) cm. (e)-(h) Corresponding B_θ contour plots. (i)-(l) Total electron density contour plots, with the erosion gap and magnetic insulation visible at $t = 34.5$ and 39 ns. The eleven contour lines range logarithmically from 10^{11} to 3×10^{13} cm⁻³. (m)-(p) Total flux vector field, $-j_e + Z j_z$.

Denser background plasma gives more pronounced jets

High Impedance Multigap Plasma Opening Switches

Rodney J. Mason, *Senior Member, IEEE*

US005568019A

United States Patent (19) (11) Patent Number: **5,568,019**
Mason (45) Date of Patent: **Oct. 22, 1996**

[54] **MULTI-GAP HIGH IMPEDANCE PLASMA OPENING SWITCH** 4,721,889 1/1988 Seidel et al. 315244 X
4,727,298 2/1988 Mendel 315244 X
5,048,068 9/1991 Turdi 315244 X
5,132,597 7/1992 Goshel et al. 315244 X
5,336,975 8/1994 Goshel et al. 315244 X

[75] Inventor: **Rodney J. Mason, Los Alamos, N.M.**

[73] Assignee: **The Regents of University of California, Oakland, Calif.**

[21] Appl. No.: 349,337
[22] Filed: Dec. 5, 1994

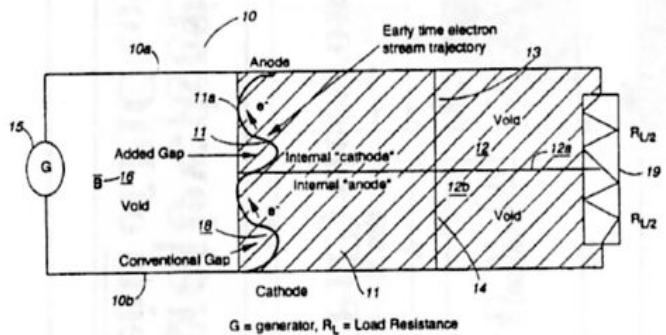
[51] Int. Cl.⁶ H01J 11/04
[52] U.S. CL. 315/344; 315/338; 315/340; 315/111.21; 315/111.41; 313/231.21

[58] Field of Search 315/111.21, 111.01, 315/111.41, 338, 340, 344; 313/157, 231.31, 298

[56] References Cited
U.S. PATENT DOCUMENTS
4,194,143 3/1990 Furtak et al. 315241 R
4,317,068 3/1992 Ward et al. 315209 CD
4,596,945 6/1996 Schumaker et al. 315244

[57] **ABSTRACT**
A high impedance plasma opening switch having an anode and a cathode and at least one additional electrode placed between the anode and cathode. The presence of the additional electrodes leads to the creation of additional plasma gaps which are in series, increasing the net impedance of the switch. An equivalent effect can be obtained by using two or more conventional plasma switches with their plasma gaps wired in series. Higher impedance switches can provide high current and voltage to higher impedance loads such as plasma radiation sources.

10 Claims, 6 Drawing Sheets



At initial $3 \times 10^{14} \text{ e-/cm}^3$ breakthrough favors the anode regions

Multiple gaps generate multiple jets – voltage adds across a load

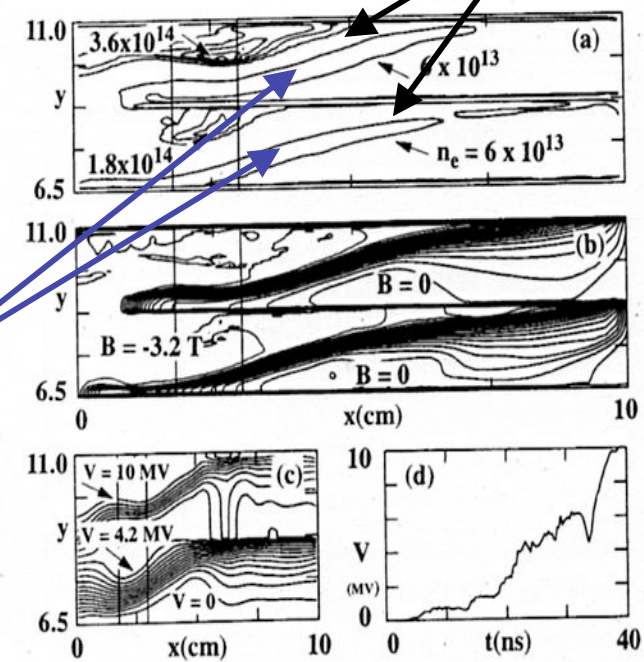
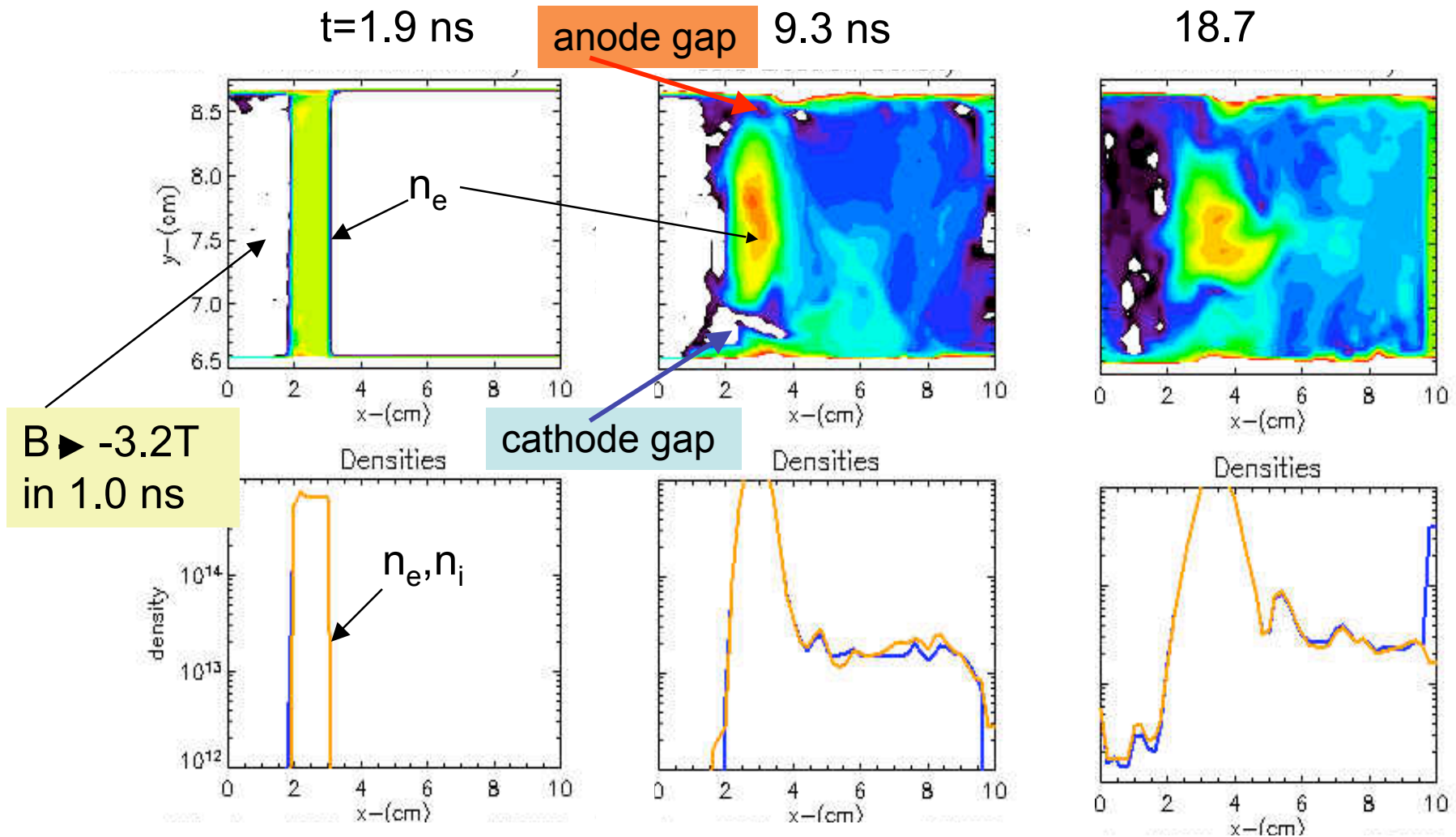


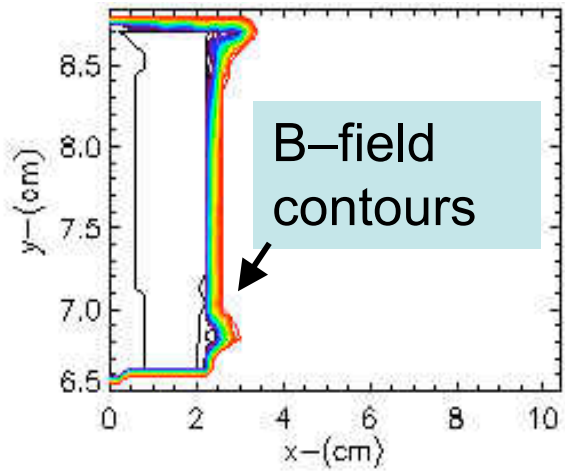
Fig. 3. Evolution at $t = 40 \text{ ns}$ with an additional internal electrode – contour intervals as in Fig. 2: (a) $n_e(x, y)$, (b) $B(x, y)$, (c) $V(x, y)$, (d) V_{load} versus

Early-time ePLAS calculations of $6 \times 10^{14}/\text{cm}^3$ C^{++} fill plasma slab show slow jets production

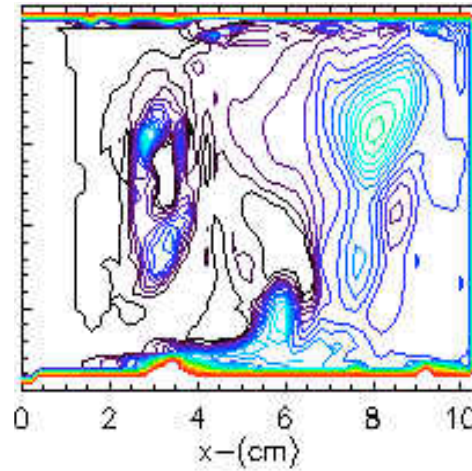


We see B-field penetration around the deformed low density plasma fill slab

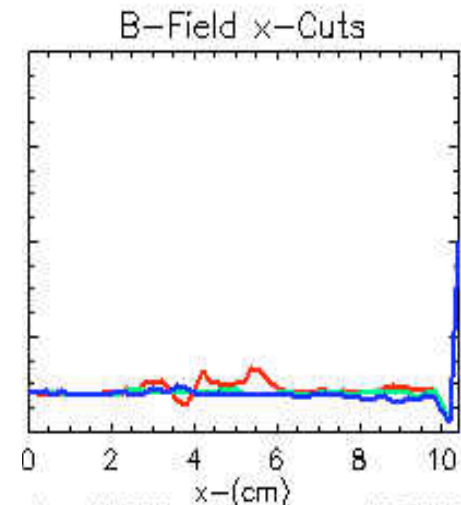
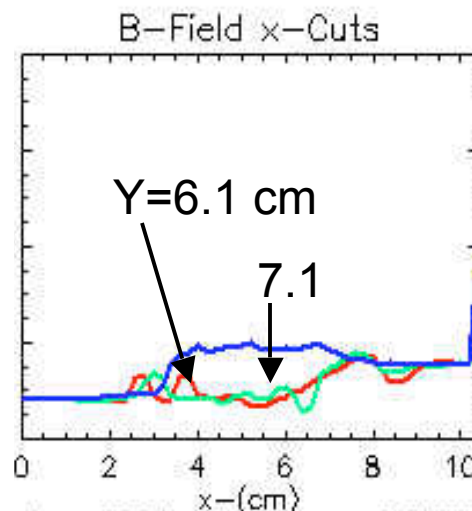
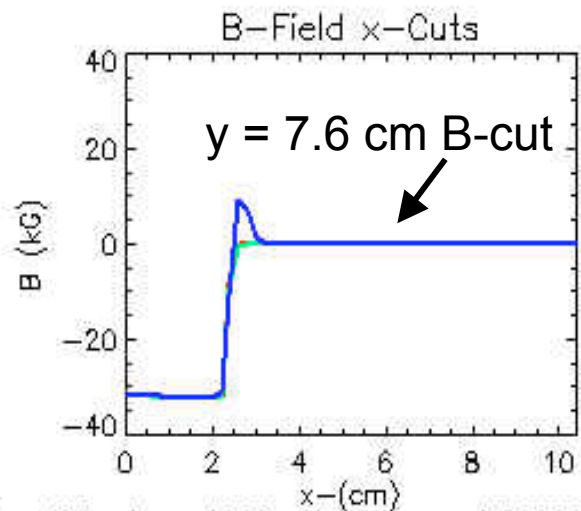
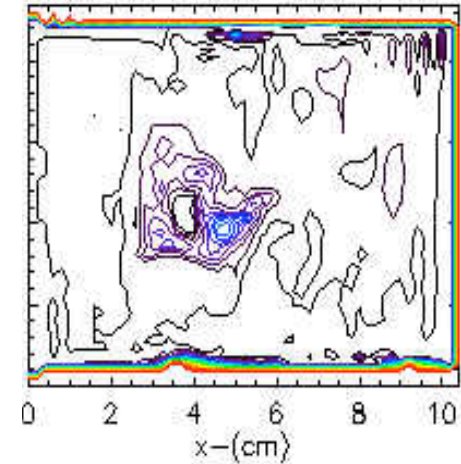
t=1.8 ns



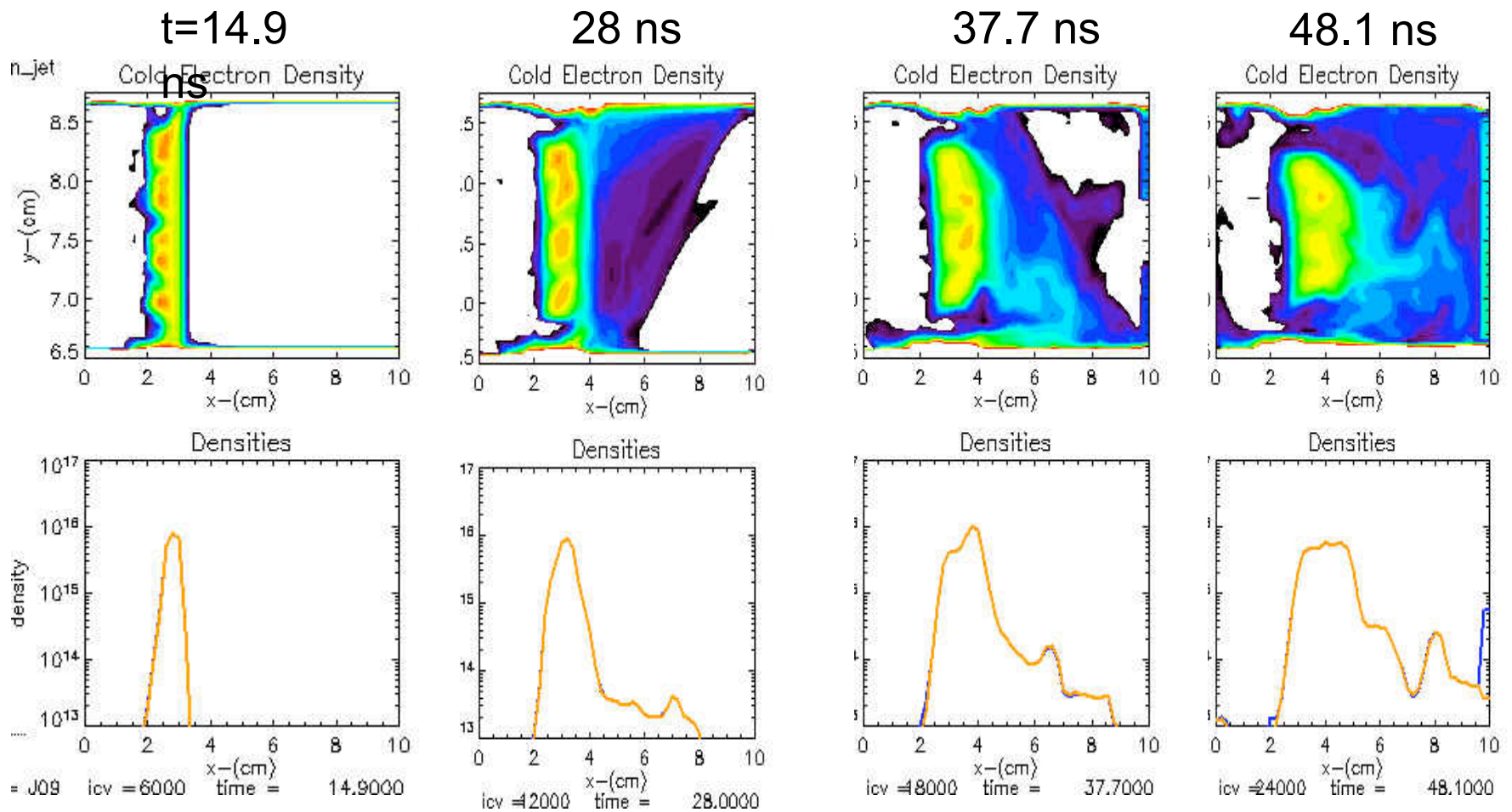
9.3



18.7



At $6 \times 10^{15}/\text{cm}^3$ the denser slab persists for longer, issuing a weak jet from the cathode



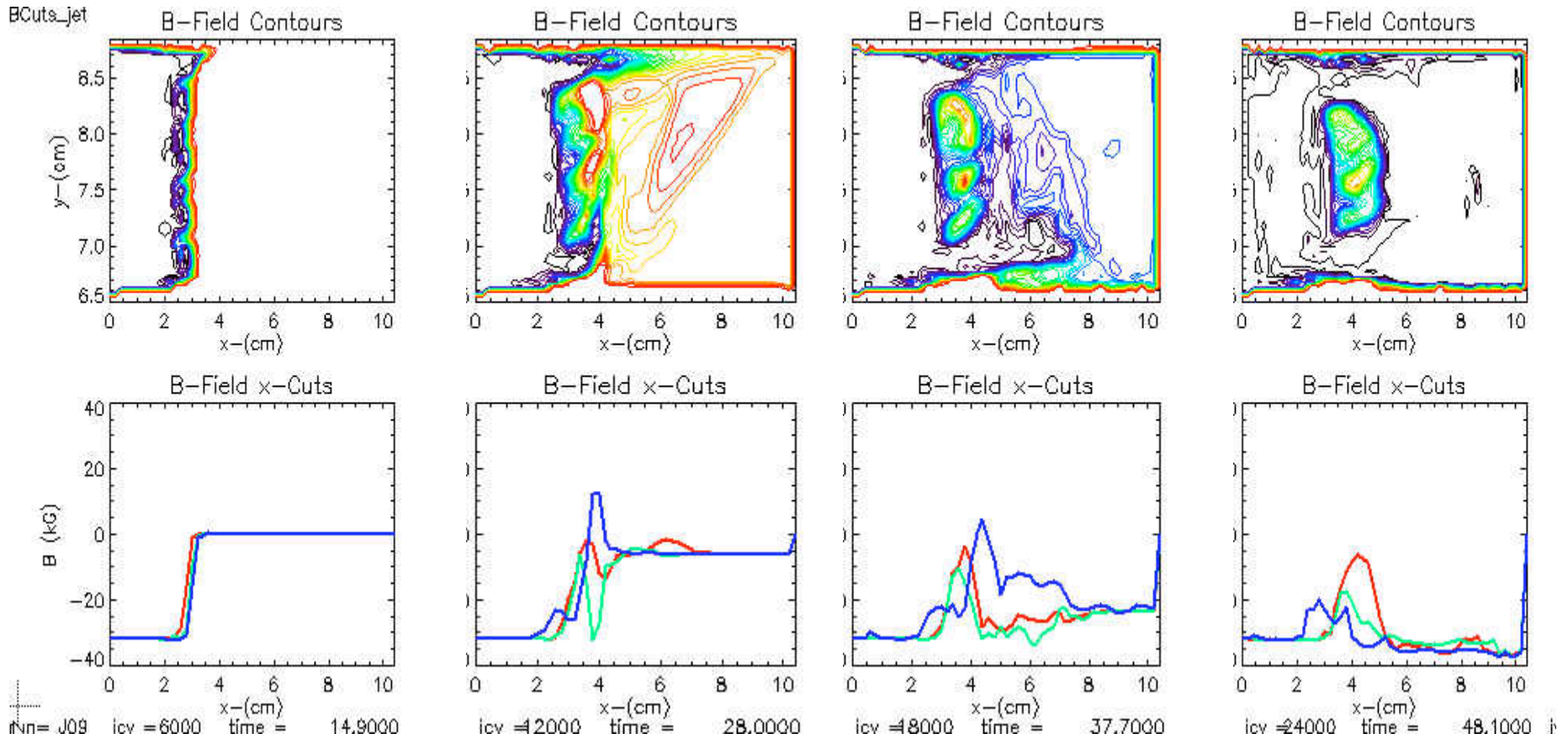
This denser slab is B-penetrated more slowly – but still manifests significant field by-pass

t=14.9 ns

28 ns

37.7

48.1



3D “shadeplots” clarify B-penetration and early plasma breakthrough at $6 \times 10^{15}/\text{cm}^3$ densities

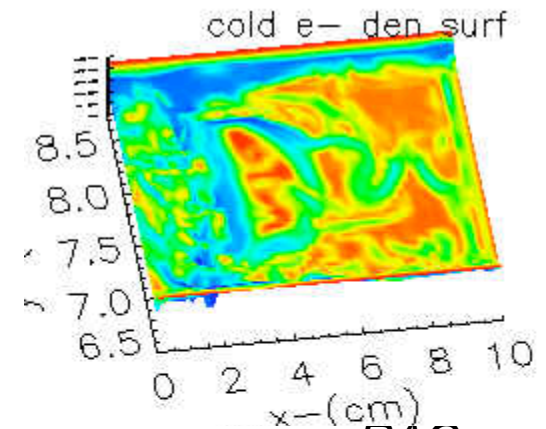
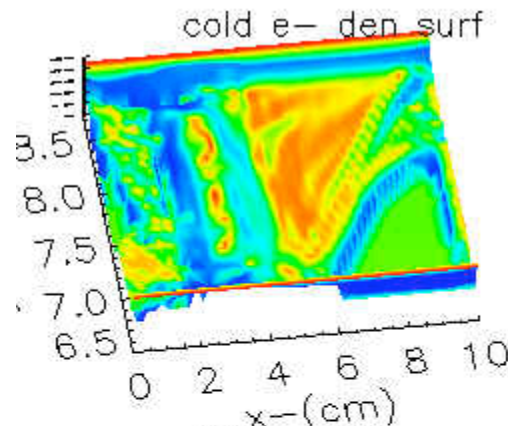
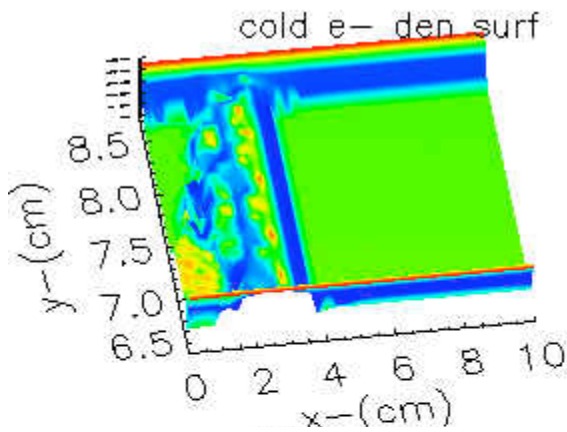
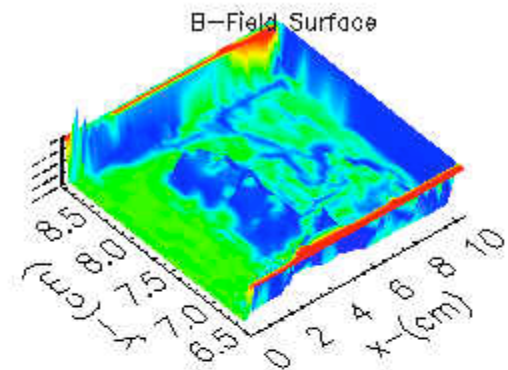
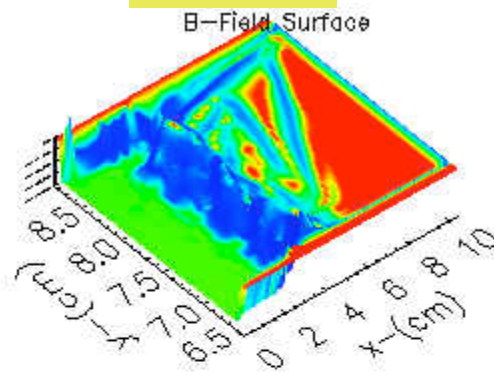
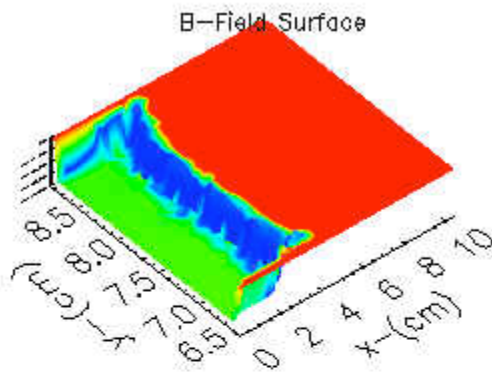
t=14.9 ns

28 ns

48.1 ns

B-field

Electron density



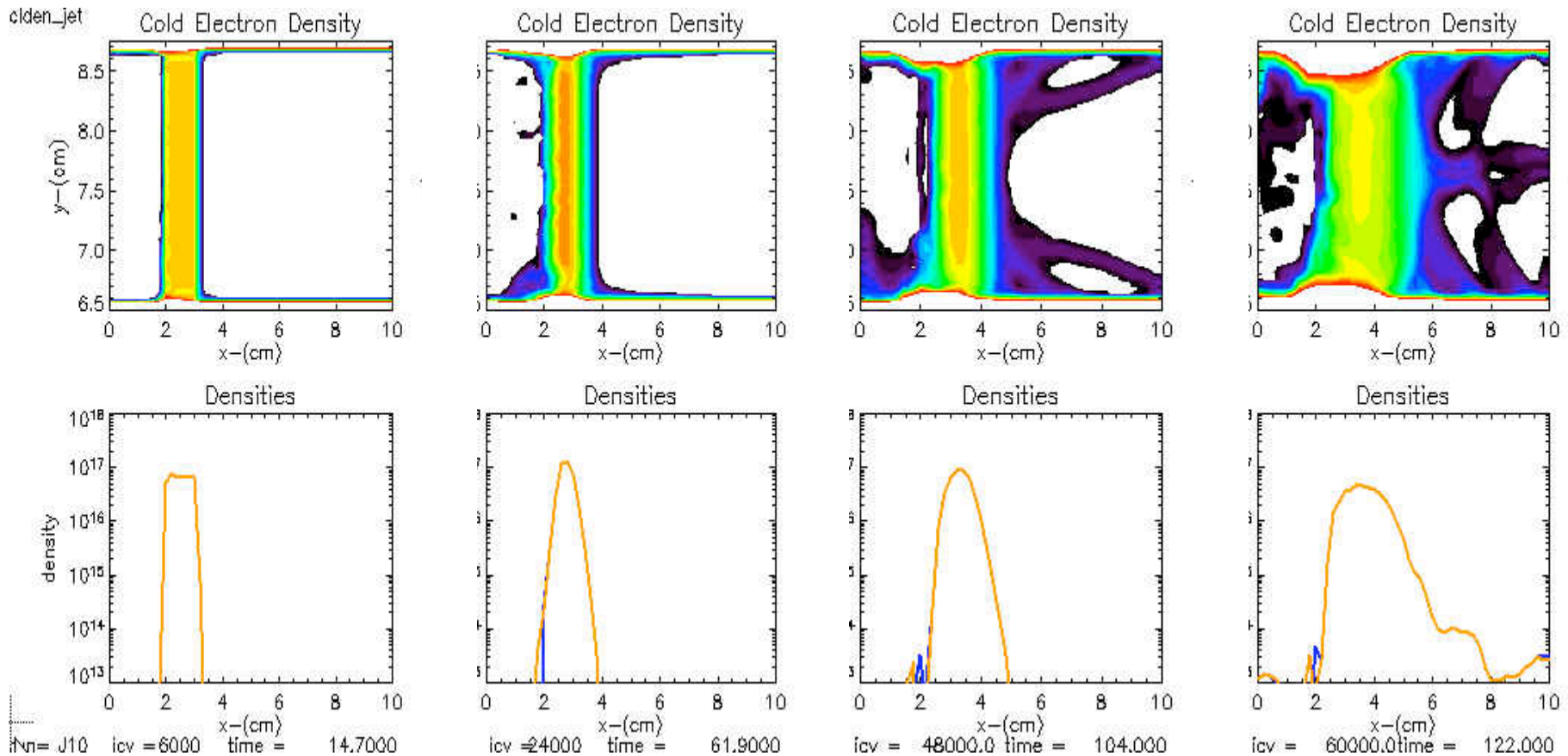
At $6 \times 10^{16} \text{ cm}^3$ B-penetration still persists at the anode and cathode, but a “solid” slab remains

t=14.7 ns

61.9 ns

104 ns

122 ns

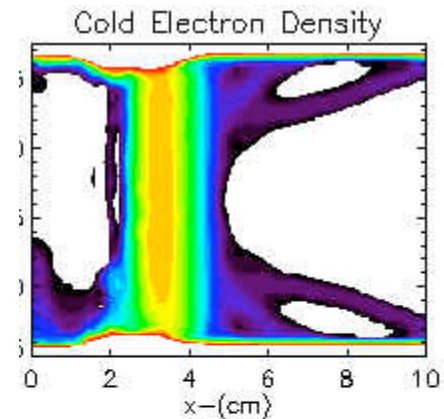
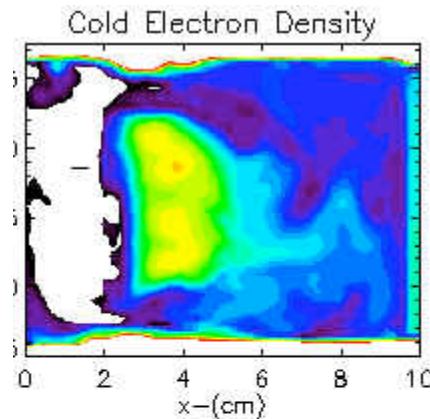
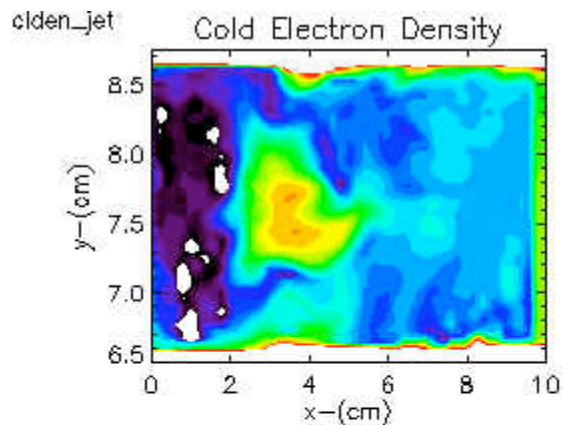
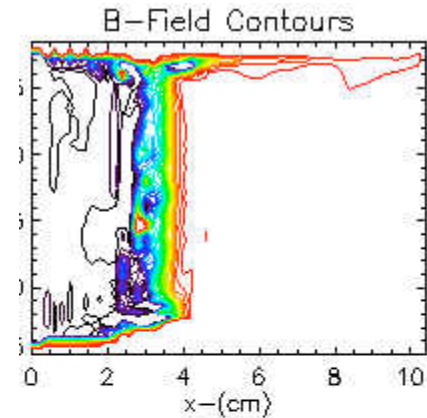
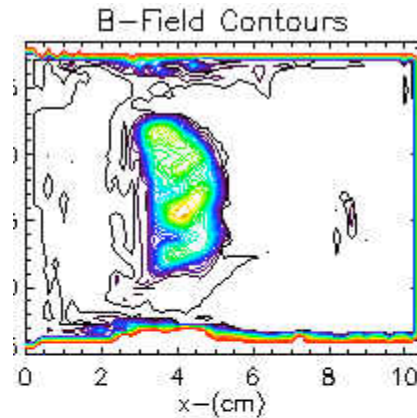
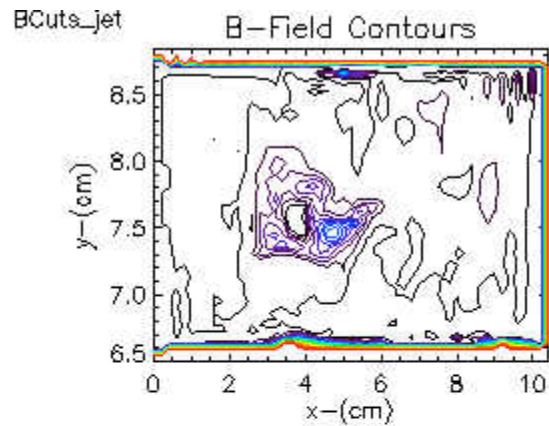


Progressively, as the slab plasma density is increased we see:

$6 \times 10^{14}/\text{cm}^3$

6×10^{15}

6×10^{16}



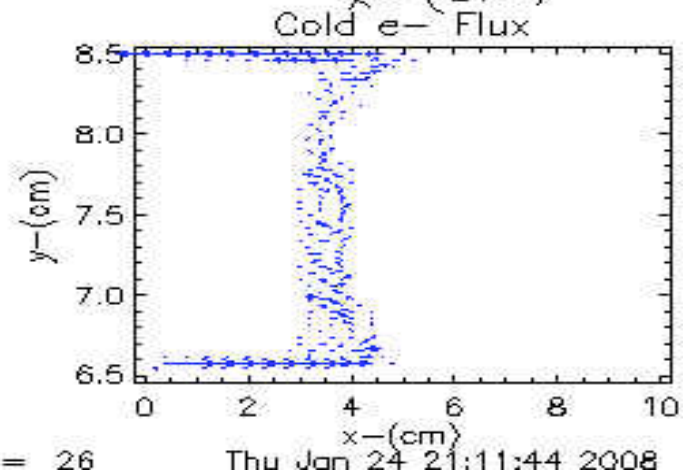
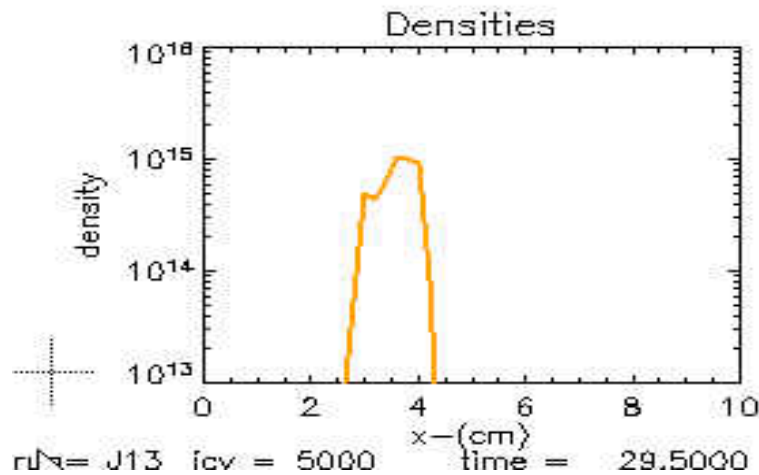
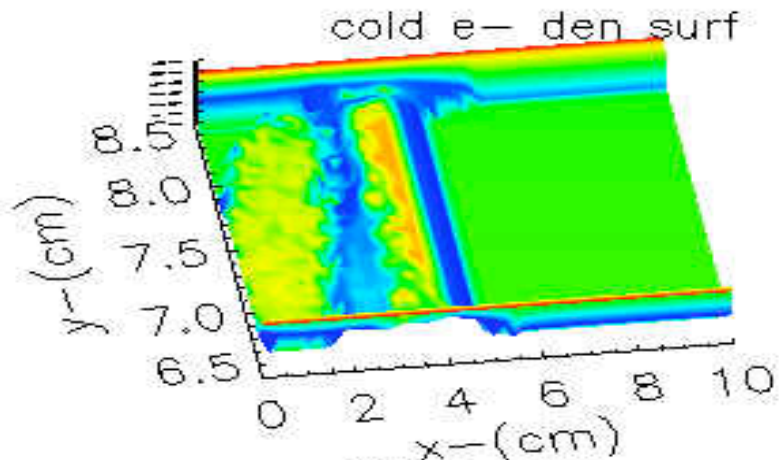
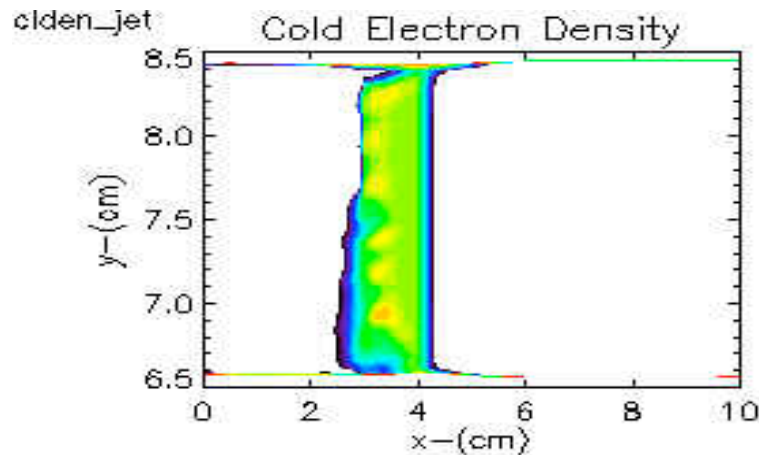
Observations

- **The $6 \times 10^{16} / \text{cm}^3$ results were run to study early HyperV modeling conditions (APS-DPP-06).**
- **These ePLAS calculations indicated sensitivity to the electron flow near the electrodes.**
- **60,000 time steps (2 hrs on a 2.8 GHz PC) were required with the explicit electron fluid treatment employed.**
- **We are now developing an implicit electron fluid treatment that should speed such calculations by 50-fold.**

Last night we explored a weaker drive B-field to better match HyperV experience (*now cyl geom*)

$B_{\max} = 3.0 \text{ kG}$ at 0.5 ns, $n_{\text{slab}}(t=0) = 10^{15}/\text{cm}^3$

$t = 29.5 \text{ ns}$

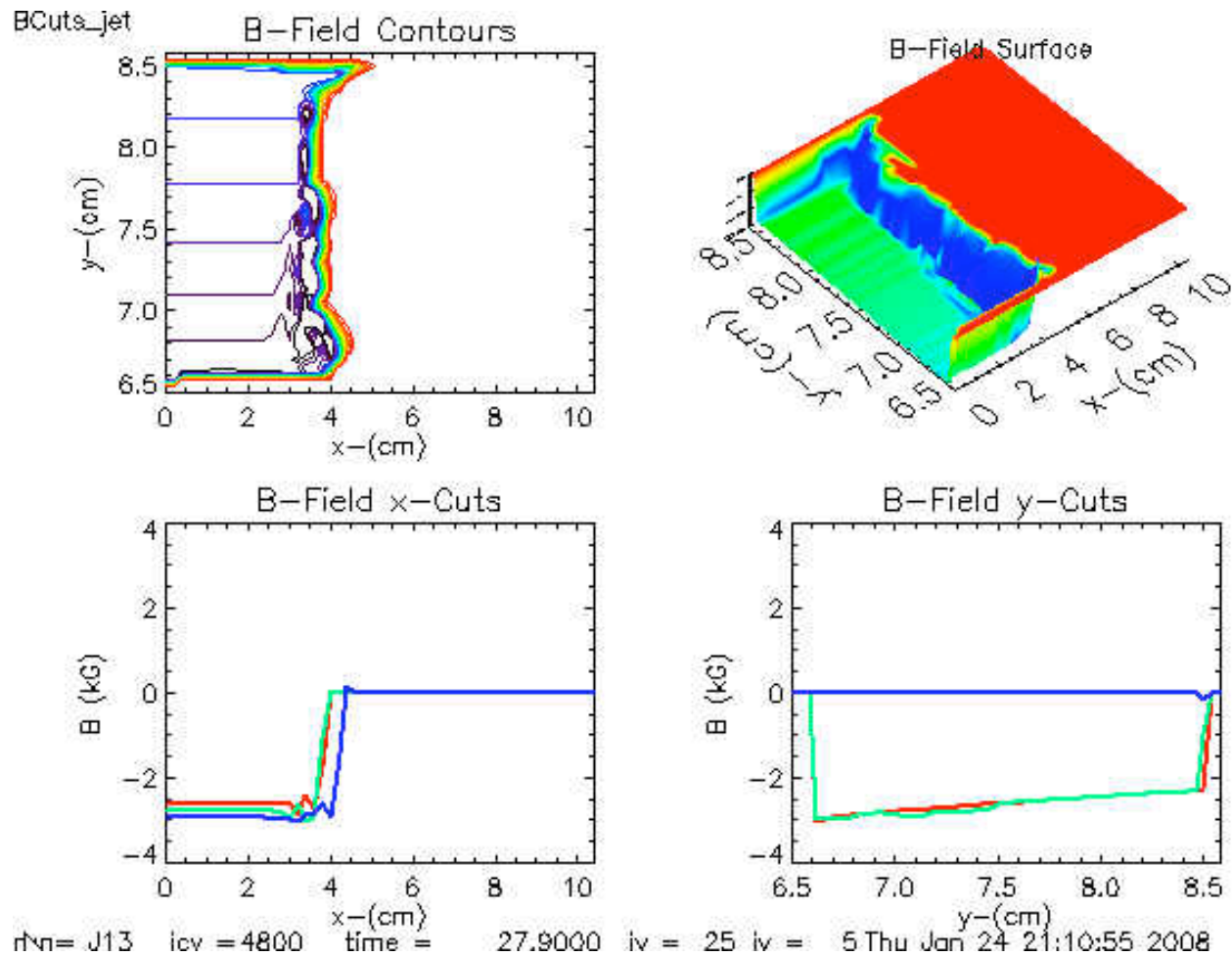


run = J13 icv = 5000 time = 29.5000

iv = 26

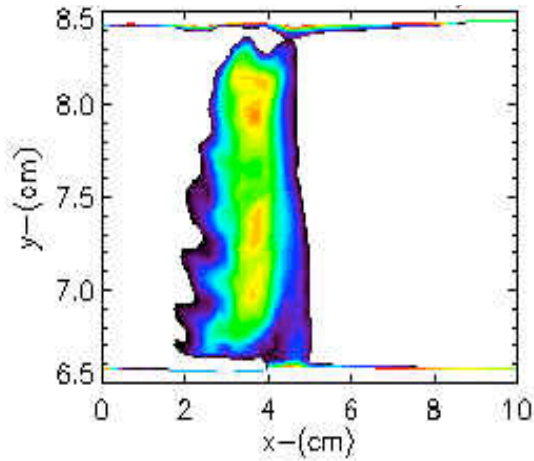
Thu Jan 24 21:11:44 2008

This is accompanied by the B-field conditions

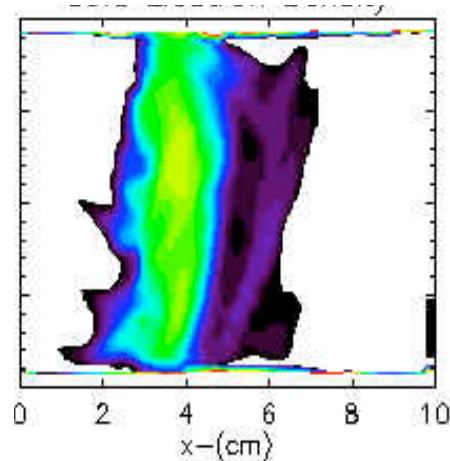


With this lower B-drive we see reduced electrode effects (using 34 min of PC time)

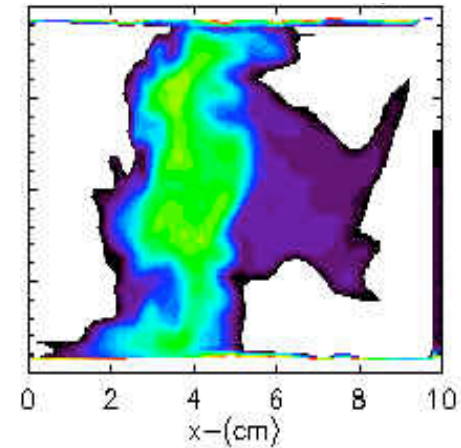
t=60.9 ns



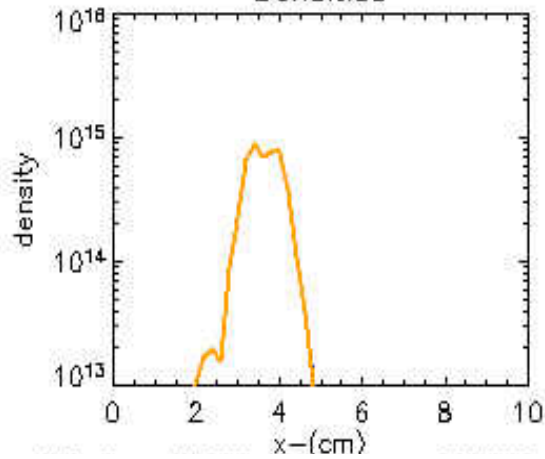
94.3 ns



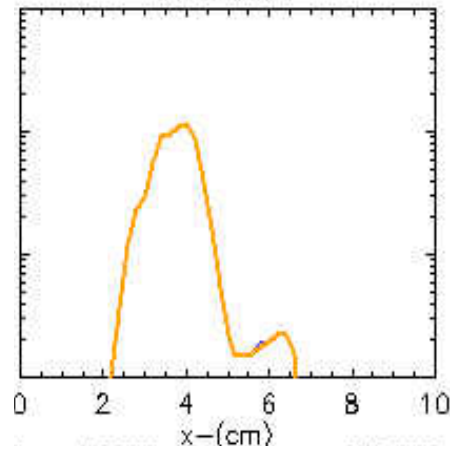
132 ns



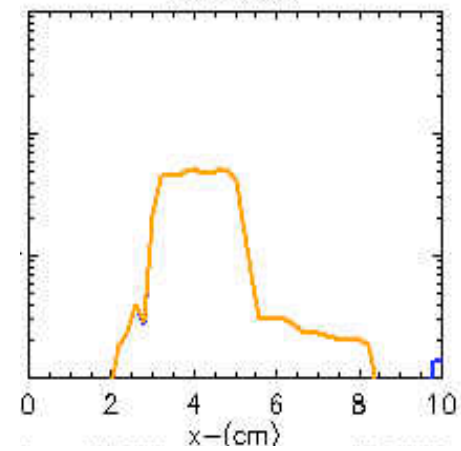
Densities



Densities



Densities



Conclusions

- **Much longer simulations are needed to follow the full development of the $10^{15}/\text{cm}^3$ slab jets.**
- **Yet, the ePLAS approach promises potentially economical insight into the dynamics of plasma jet generation.**
- **Implicit plasma simulation permits the modeling of plasma jets spanning a broad range of densities.**
- **Wall emission limitation (e.g. erosion) remains a concern limiting momentum transfer to the jets.**
- **An implicit (or pseudo-massless) fluid electron treatment is needed to accelerate microsecond modeling.**